Acc. Sc. Torino
Memorie Sc. Fis. 33 (2009)

Piezonuclear neutrons from brittle fracture: early results of mechanical compression tests

Memoria di ALBERTO CARPINTERI[*], FABIO CARDONE[**] e GIUSEPPE LACIDOGNA[*]
presentata dal Socio nazionale Alberto CARPINTERI
nell'adunanza del 10 dicembre 2008

Abstract. *Neutron emission measurements by means of helium-3 neutron detectors were performed on solid test specimens during crushing failure. The materials used were marble and granite, selected in that they present a different behaviour in compression failure (i.e., a different brittleness index) and a different iron content. All the test specimens were of the same size and shape. Neutron emissions from the granite test specimens were found to be of about one order of magnitude larger than the natural background level at the time of failure. These neutron emissions were caused by piezonuclear reactions that occurred in the granite, but did not occur in the marble. This is due to the fact that in granite the release rate of accumulated elastic energy ΔE exceeds the power threshold for the generation of piezonuclear reactions, $W_{strong} = 7.69\times10^{11}$ W. Moreover, granite contains iron, which has been ascertained to be the most favourable element for the production of piezonuclear reactions when the nuclear interaction energy threshold, $E_{0,\ strong} = 5.888\times10^{-8}$ J, is exceeded in deformed space-time conditions.*

Keywords: neutron emission, piezonuclear reactions, rocks crushing failure, catastrophic failure, size-scale effects in compression.

Riassunto. *Sono state eseguite misure di emissione di neutroni con rivelatori ad elio3 in materiali solidi sottoposti a frantumazione. I due materiali usati sono stati il marmo ed il granito, poiché presentano un diverso comportamento rispetto alla rottura per compressione (ossia hanno un differente indice di fragilità) e poiché differiscono nel contenuto di ferro. I campioni sono stati presi tutti con uguali dimensioni e forma. Solo nel granito sono state misurate emissioni di neutroni di circa un ordine di grandezza superiori al fondo naturale nel momento della rottura. I neutroni emessi sono stati conseguenza di reazioni piezonucleari che si sono verificate nel granito, ma non nel marmo. Le reazioni piezonucleari sono state causate dal fatto che nel granito*

[*] Department of Structural Engineering and Geotechnics, Politecnico di Torino, Corso Duca degli Abruzzi 24, 10129 Turin, Italy.
[**] ISMN – CNR Via dei Taurini 19, 00187 Rome, Italy.

la velocità di rilascio dell'energia elastica accumulata ΔE è risultata superiore alla potenza di soglia per la produzione di reazioni piezonucleari $W_{strong} = 7.69 \times 10^{11}$ *W, mentre nel marmo è stata inferiore. Inoltre il granito contiene ferro, che si è dimostrato essere l'elemento più favorevole nella produzione di reazioni piezonucleari in presenza del superamento, in condizioni di spazio-tempo deformato, della soglia energetica di interazione nucleare* $E_{0,\,strong} = 5.888 \times 10^{-8}$ *J.*

Parole chiave: emissione di neutroni, reazioni piezonucleari, frantumazione delle rocce, rottura catastrofica, effetti di scala in compressione.

1. Introduction

From the studies by Diebner [1], Kaliski [2] and Winterberg [3], it is known that piezonuclear reactions can be obtained in solid radioactive materials in which neutron production is catalysed by pressure. Later on, Arata [4] conducted experiments showing the possibility of piezonuclear reactions taking place in gaseous materials made up of deuterium gas, and Taleyarkhan [5] showed that neutron emitting piezonuclear reactions may occur in deuterium-containing liquids with radioactive substances dissolved in them. Finally, piezonuclear reactions with neutron emissions were produced in iron-containing inert liquids without deuterium and without radioactive substances [6-8]. Accordingly, tests were conducted to assess neutron production from piezonuclear reactions in solids subjected to compression till failure. These experiments are based on the following phenomenological analogy. In the tests described in [5,7-8], the pressure of ultrasonic waves in a liquid was seen to cause the cavitation of the gasses dissolved therein, resulting in the speed of energy threshold for nuclear interaction W_{strong} being exceeded, with the ensuing production of piezonuclear reactions [6,5] and neutron emissions. It was hypothesized that the fracture of solid materials were able to reproduce the cavitation conditions of liquids and hence lead to the production of piezonuclear reactions, provided that the materials were properly selected. The materials selected for the tests were Carrara marble (calcite) and green Luserna granite (gneiss). This choice was prompted by the consideration that, test specimen dimensions being the same, different brittleness numbers [9] would cause catastrophic failure in granite, not in marble. The test specimens were subjected to uniaxial compression to assess scale effects on brittleness [10]. Four test specimens were used, two made of Carrara marble, consisting mostly of calcite, and two made of Luserna granite, all of them measuring 6x6x10 cm^3 (Fig. 1). The same testing machine was used on all the test specimens: a standard servo-hydraulic press with a maximum capacity of 500 kN, equipped with control electronics (Fig. 1b). This machine makes it possible to carry out tests in either load control or displacement control. The tests were performed in piston travel displacement control by setting, for all the test specimens, a velocity of 10^{-6} m/s during compression. Neutron emission measurements were made by means of a he-

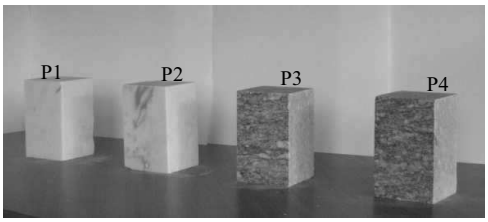

a

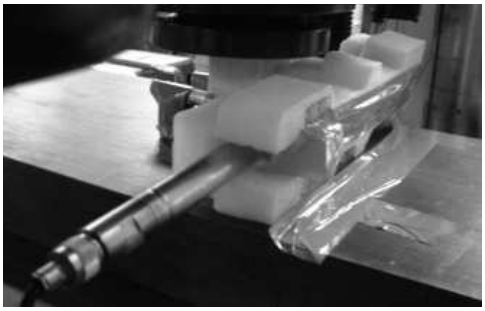

c

b

Figure 1: The test specimens analysed, two in Carrara marble (P1, P2) and two in Luserna granite (P3, P4), measuring 6x6x10 cm^3 (a). Baldwin servo-controlled press used for the compression tests (b). Helium-3 neutron detector placed in the proximity of test specimen P1 during the test. The detector is enclosed in a polystyrene case for protection against possible impacts due to test specimen failure (c).

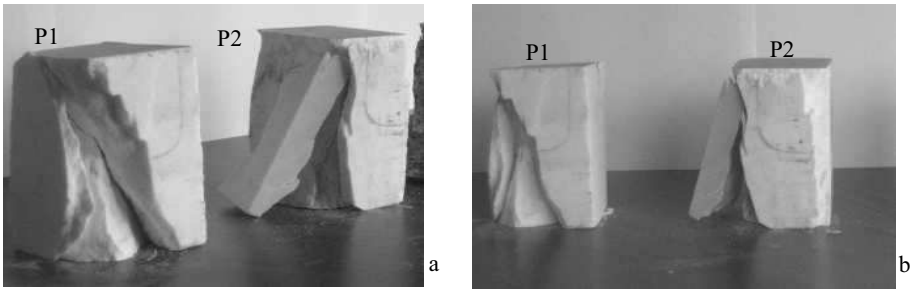

Figure 2: Views (a) and (b) of test specimens P1 and P2 in Carrara marble following compression failure.

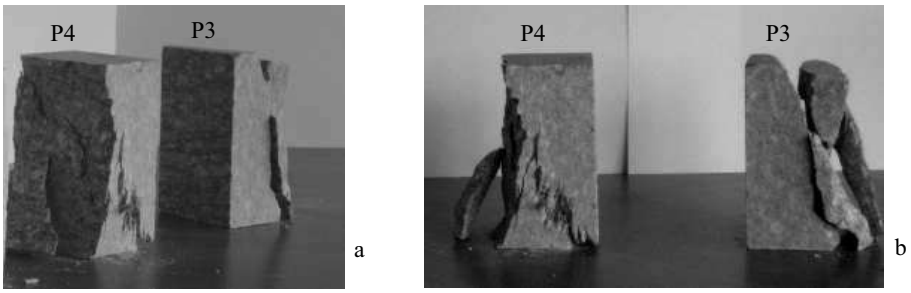

Figure 3: Views (a) and (b) of test specimens P3 e P4 in Luserna granite following compression failure.

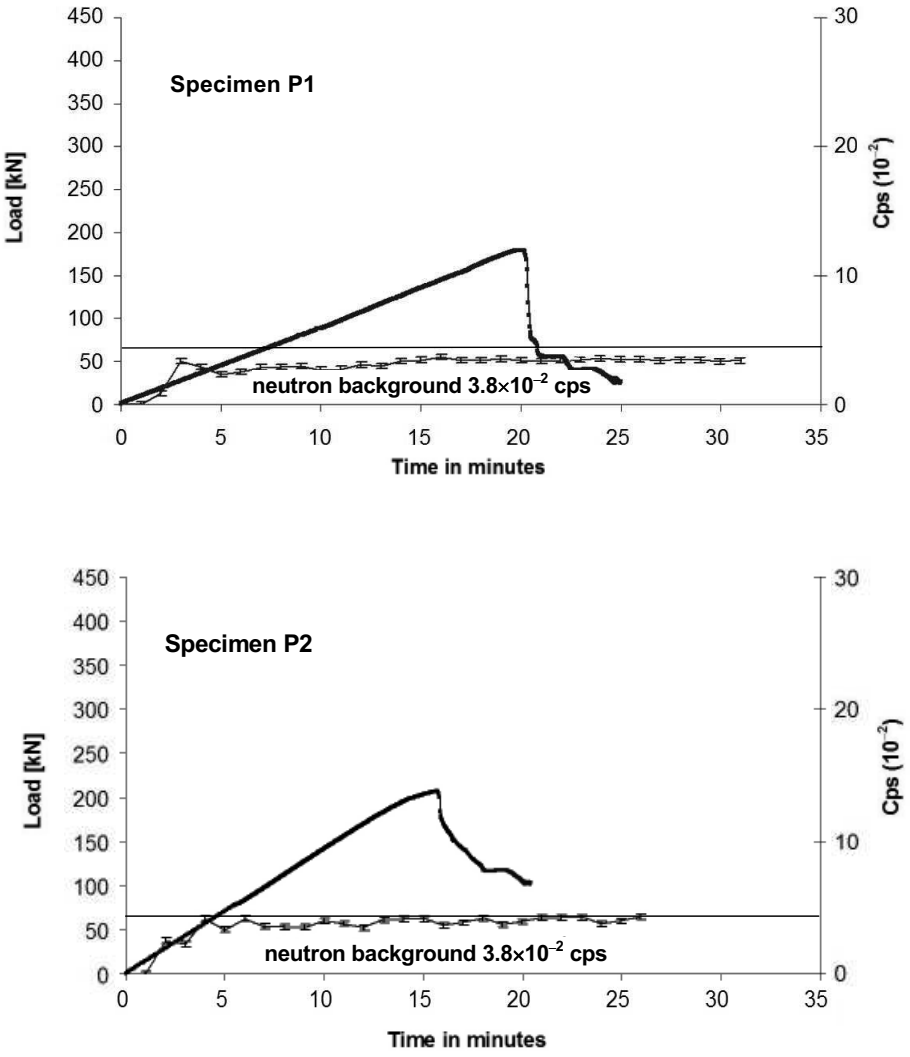

Figure 4: Load vs. time and cps curves for P1 and P2 test specimens in Carrara marble.

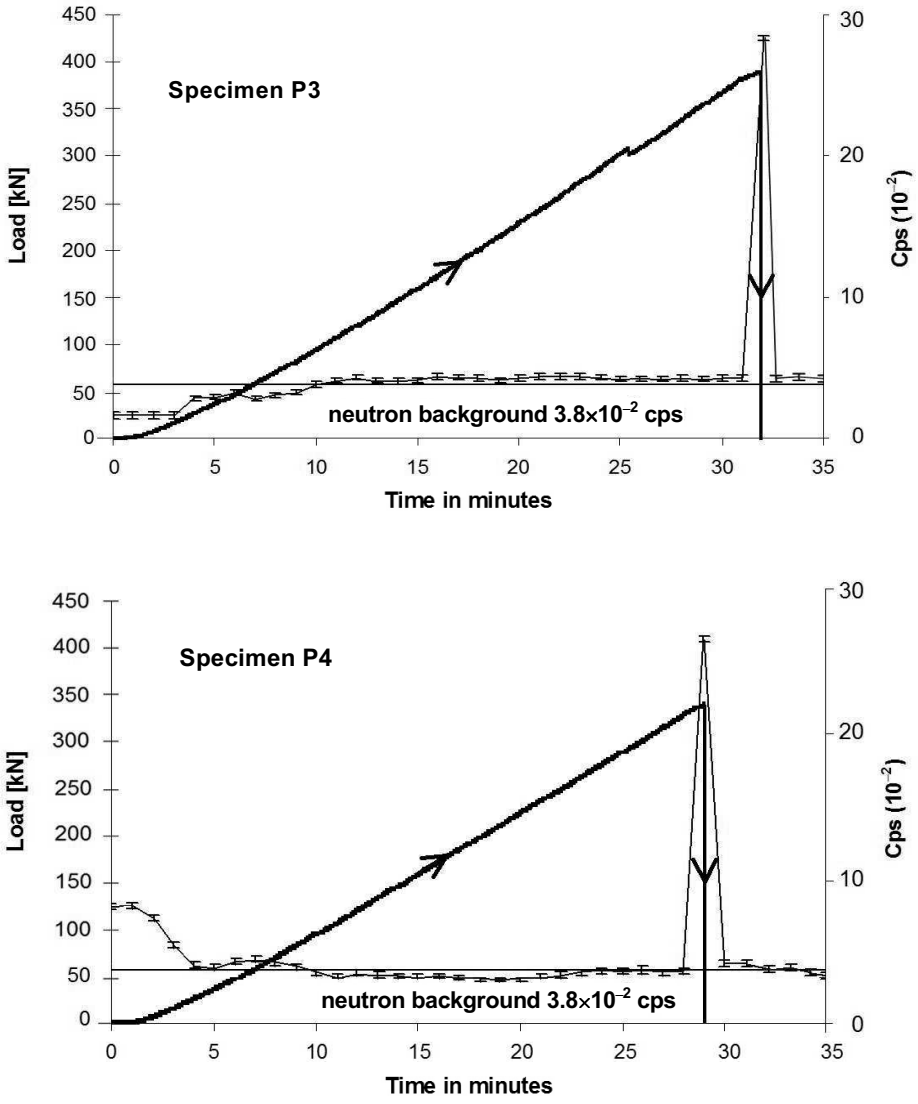

Figure 5: Load vs. time and cps curves for test specimens P3 and P4 in Luserna granite.

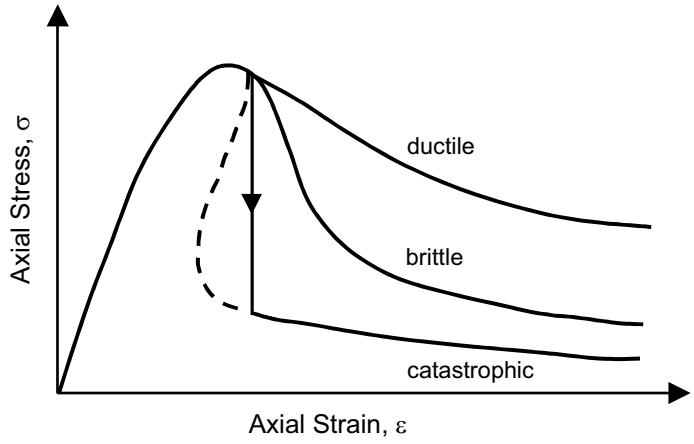

Figure 6: Ductile, brittle and catastrophic behaviour.

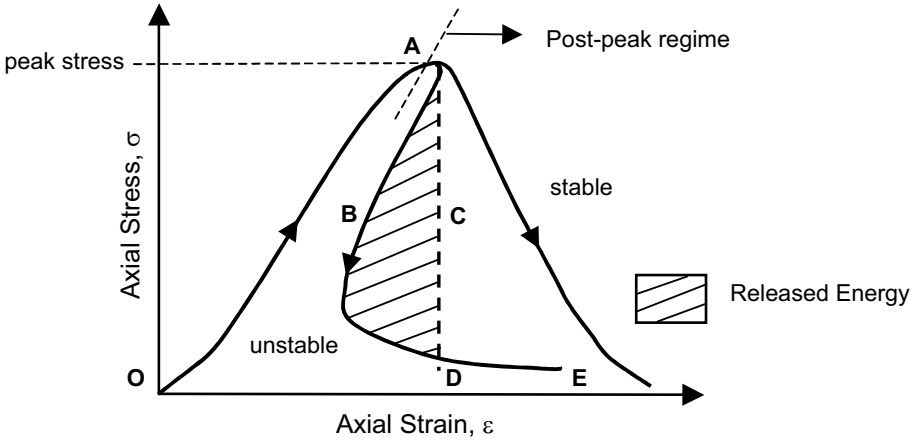

Figure 7: Energy release and stable vs. unstable stress-strain behaviour.

lium-3 detector placed at a distance of 10 cm from the test specimen and enclosed in a polystyrene case so as to prevent the results from being altered by acoustical-mechanical stresses (Fig. 1c). During the preliminary tests, thermodynamic neutron detectors of the bubble type BD (bubble detector/dosimeter) manufactured by Bubble Technology Industries (BTI) were used, and the indications obtained persuaded us to carry on the tests also with helium-3 detectors.

2. Experimental set-up

2.1 The servo-hydraulic press

The servo-controlled press employed works by means of a digital type electronic control unit. The management software is TestXpertII by Zwick/Roel, while the mechanical parts are manufactured by Baldwin (Fig. 1b). The force applied is determined by measuring the pressure in the loading cylinder by means of a transducer. The margin of error in the determination of the force is 1%, which makes it a Class 1 mechanical press. The stroke of the press platen in contact with the test specimen is controlled by means of a wire type potentiometric displacement transducer.

2.2 The neutron detector

The neutron detector used in the tests is a helium-3 type with electronics of preamplification, amplification and discrimination directly connected to the detector tube, which is of the type referred to as “long counter”. The helium-3 gas supplies the neutron detection signal through the phenomenon of recoil protons from the anelastic scattering of the neutrons against the nuclei of the helium-3 atoms; the protons supply the electric signal which is read by the electronics equipping the detector. Low-voltage power for the detector electronics is supplied via a NIM (Nuclear Instrument Module); this is a standard device for the electronics used in nuclear physics applications for the management of the circuits dealing with the electric signals generated by a radiation detector. The helium-3 detector is powered with 1.3 kV, supplied via a high voltage NIM. The signal reading electronics analog output is analysed during the tests by means of an oscilloscope, to keep the signal shape under control. The logic output producing the TTL pulses is connected to a NIM counter. The logic output of the detector is enabled for analog signals exceeding 300 mV. This discrimination threshold is a consequence of the sensitivity of the helium-3 detector to the gamma rays ensuing neutron emission in ordinary nuclear processes. This value was determined by measuring the analog signal of the detector by means of a Co-60 gamma source. This detector was also calibrated for the measurement of thermal neutrons; its sensitivity is 65 cps/$n_{thermal}$, i.e., the fluency rate of thermal neutrons was 1 thermal neutron/s cm^2, corresponding to a count rate of 65 cps. The neutron

background was measured at 600 s time intervals to obtain sufficient statistical data with the detector in the position shown in Fig. 1c. The average background count rate was:

$$3.8\times10^{-2} \pm 0.2\times10^{-2} \text{ cps}$$

corresponding to an equivalent flux of thermal neutrons of

$$5.8\times10^{-4} \pm 0.3\times10^{-4} \text{ n}_{\text{thermal}}/\text{s cm}^2.$$

3. The tests

Neutron emissions were measured on four test specimens, two made of marble, denoted with P1, P2, and two of granite, denoted with P3, P4 (see Fig. 1a). The test specimens were arranged with the two smaller surfaces in contact with the press platens , with no coupling materials in-between, according to the testing modalities known as "test by means of rigid platens with friction". The mass and density of each marble and granite test specimen are given in Table 1.

Table 1: Physical characteristics of the test specimens.

Test specimens	Dimensions [cm3]	Material	Weight [g]	Density [g/cm3]
P1	6x6x10	Carrara marble	950	2.64
P2	6x6x10	Carrara marble	946	2.62
P3	6x6x10	Luserna granite	882	2.45
P4	6x6x10	Luserna granite	836	2.32

The electronics of the neutron detector were powered at least 40 minutes before starting the compression tests to make sure that the behaviour of the device was stable with respect to intrinsic thermal effects. Then, background measures were repeated for 600 s to make sure there were no variations. The acquisition time was fixed at 60 s and the results of count rate measurements are given in Figs. 4 and 5 together with the diagrams of the force applied to the test specimens as a function of the time elapsed since the beginning of its application.

4. Neutron emission measurements

The measurements of neutron emissions obtained on the marble test specimens yielded values comparable with the background, even at the time

of test specimen failure. Figure 2 shows two views of the marble test specimens after failure. The neutron measurements obtained on the two granite test specimens, instead, exceeded the background value by about one order of magnitude at the test specimen failure. Two views of the granite test specimens after failure can be seen in Fig. 3.

After 20 min, test specimen P1 reached a peak load of ca 180 kN, corresponding to an average pressure on the bases of 50 MPa; after 15 min, test specimen P2 reached a peak load of ca 200 kN, corresponding to an average pressure on the bases of 55.6 MPa.

Test specimen P3 reached at time T(P3) = 32 min a peak load of ca 400 kN, corresponding to an average pressure on the bases of 111.1 MPa. When failure occurred, the count rate was found to be

$$28.3\times10^{-2} \pm 0.2\times10^{-2} \text{ cps}$$

corresponding to an equivalent flux of thermal neutrons of

$$43.6\times10^{-4} \pm 0.3\times10^{-4} \text{ } n_{thermal}/\text{s cm}^2.$$

Test specimen P4 reached at time T(P4) = 29 min a peak load of ca 340 kN, corresponding to an average pressure on the bases of 94.4 MPa. When failure occurred, the count rate was found to be

$$27.2\times10^{-2} \pm 0.2\times10^{-2} \text{ cps}$$

corresponding to an equivalent flux of thermal neutrons of

$$41.9\times10^{-4} \pm 0.3\times10^{-4} \text{ } n_{thermal}/\text{s cm}^2.$$

Notice how the above neutron measurements occurring in P3 and in P4 failure are well beyond the background interval and how the value obtained on P3 is greater than the value measured on P4. We believe that this event, albeit with the due caution, may be ascribed to the unstable failure of these test specimens and the greater quantity of energy released by P3 compared to P4 at the time of failure. Figures 4 and 5 summarise the evolution of the neutron count rates together with the load vs. time curves for the four test specimens.

5. Factors involved in controlling rock failure

Experimental data from rocks tested in compression generally indicate that this is a brittle material, since it exhibits a rapid decrease in load carrying capacity when deformed beyond a peak load. When the softening diagram is very steep, or even shows simultaneously decreasing strain and stress values, the material is said to present a snap-back or catastrophic be-

haviour. This is in contrast with ductile materials which retain considerable strength beyond the peak as shown in Fig. 6.

Even though in the post-peak phase the load-carrying capacity of the material may decrease considerably with increasing strain (i.e. the material "softens"), in actual practice this behaviour can be important to the overall performance of a rock or concrete structure.

In laboratory studies, the external loading system is the testing machine. Depending on its design, the machine may have a relatively soft or stiff characteristic compared to the test specimen. A stiff frame and electronic servo-controls are required in order to observe the post-failure behaviour of brittle materials [12].

By programming a linear increase in axial displacement with time, the complete stress-strain curve for rock is obtained (Fig. 7). Generally, strains increase linearly with time even though the specimens fail and the system undergoes a progressive reduction in load-bearing capacity during the process. Such specimens are said to exhibit stable failure characteristics.

However, if the complete stress-strain curve does not monotonically increase in strain, the linear increase can only be achieved along the OACDE curve shown in Fig. 7. Since the material behaviour is represented by the OABDE curve, excess energy, proportional to the shaded area, is released by the specimen and the result is uncontrolled violent failure. Such specimens are said to exhibit unstable failure characteristics.

This suggests that certain types of catastrophic failure cannot be controlled without feedback control of the testing machine. According to this principle, the control of rocks failure is optimized when the feedback transducer is located for maximum sensitivity in detecting failure. In such uniaxial compression tests the displacement transducer will be most sensitive to failure development if it is mounted in the direction perpendicular to the loading axis. Only in this conditions is it possible to control rock failure automatically when the stress-strain curve does not monotonically increase in strain [12].

In this framework, Carpinteri showed, adopting a cohesive crack model for a concrete-like material in tension, that the slope of the stress-strain response changes substantially by varying the size-scale while keeping the geometrical shape of the structure unchanged [9,10]. Controlling the loading process by displacement, the softening branch becomes steeper when the size-scale increases, and a critical size-scale exists for which the softening slope is infinite. In such a case the load carrying capacity drastically decreases for relatively small displacements increments. Then, for size-scales larger than the critical one, the softening slope becomes positive and the loading capacity will present a discontinuity with a negative jump.

Very recently the same author, by analogy with the cohesive crack model, has proposed the overlapping crack model to describe the size effects in compressed materials. For both traction and compression behaviours, the size-scale transition from ductile to brittle behaviour is governed by a non-dimensional brittleness number, s_E, which is a function of material properties and structure size-scale [9-10].

6. Size-scale effects in compression

Stable and unstable behaviours, although some materials are intrinsically more brittle than others, both depend on the specimen size and shape [9-11, 14]. The problem of the size-effect on the brittleness of heterogeneous materials such as concrete has been investigated extensively. However, it is very difficult to study this phenomenon for compression loading, since the strength and the behaviour of concrete depend to a considerable extent on friction between the specimen bases and the loading platens of the testing machine, as well as on specimen slenderness [11,14].

Size-effects also influence the post-peak softening branch of the stress-strain diagram. Experimental tests evidenced that, in the softening regime, ductility is a decreasing function of size-scale and slenderness, whereas it increases with increasing friction [13].

The stress-strain relationships usually assumed consider an energy dissipation within a volume, but they are absolutely ineffective in describing size-scale effects on specimens ductility. On the contrary, a close observation of the stress vs. post-peak deformation curves shows that a strong localization of deformations occurs in the softening regime. This suggests that, in the softening regime, energy dissipation takes place over an intermediate domain between volume and surface. In this context, the application of fractal concepts to compression behaviour gives a theoretical explanation of size-scale effects on compressive strength, as well as on dissipated energy density [10,11,14].

Thus, it can be stated that energy release modalities during compressive tests depend on the intrinsic brittleness of the material of the test specimens, as well as on test specimen dimensions and slenderness. Furthermore, it may be assumed that energy release rate also depends on the velocity setting of testing machine piston travel.

Based on the foregoing concepts, further tests could be carried out on specimens made of different materials and having different dimensions and slenderness ratios, as well as by setting different piston travel velocities. These tests would make it possible to assess the influence of size-scale and loading rate effects on energy release rate in compression, and hence on the possibility of producing neutron emissions.

7. Discussion and remarks

In this study, all compression tests were conducted through feedback control of the axial displacement of piston travel on test specimens having the same dimensions. The complete specimen collapse process was observed only for P1 and P2 marble specimens, whose behaviour was seen to be ductile compared to the brittle catastrophic failure behaviour displayed by granite specimens P3 and P4. For the latter two, in fact, failure occurred instantaneously, without showing the descending branch of the load-time curve.

By taking into account only the positive derivative branch of the load-time curves, from the evolution of the load in the four test specimens it can be seen that failure occurs when peak compressive load is reached (Figs. 4 and 5). The elastic strain energy accumulated in the test specimens up to failure, ΔE, is given in Table 2. Moreover, for each test specimen, it is possible to draw some conclusions on the release rate of the elastic energy accumulated, considering that granite displays brittle, catastrophic failure behaviour, while marble is characterised by a more ductile behaviour.

Table 2: Elastic strain energy at the peak load, ΔE .

Test specimen	Material	ΔE [J]
P1	Carrara marble	124
P2	Carrara marble	128
P3	Luserna granite	384
P4	Luserna granite	296

One of the conditions to be met for piezonuclear reactions to take place is that the ratio, r, between the power of released energy, $W=\Delta E/\Delta t$, and the power threshold [6-7]:

$$W_{strong} = 7.69\times10^{11}\ W \tag{1}$$

be greater than or equal to 1 [6-7]:

$$r = W/\ W_{strong} \geq 1. \tag{2}$$

Accordingly, based on the data obtained from the tests, the time interval of released energy, Δt, in granite test specimens in which piezonuclear reactions have occurred, should satisfy the following relationship:

$$\Delta E/\Delta t \geq W_{strong}, \tag{3}$$

and hence:

$$\Delta t \leq \frac{\Delta E}{W_{strong}} = \frac{384}{7.69 \times 10^{11}} = 0.5 \times 10^{-9}\,s = 0.5\,ns \tag{4}$$

Equation (4) was written by considering the energy accumulated in P3 which was greater than the energy accumulated in P4. For the marble test specimens, in which the peak load is clearly followed by a softening branch, energy release surely occurred over a period of time too long to permit the production of piezonuclear reactions. Accordingly, neutron emissions in granite may be accounted for by the fact that the power threshold for piezonuclear reactions is exceeded, as well as by the type of catastrophic failure that occurs, which entails a very fast energy release, over a time period of the order of a nanosecond. Furthermore, with these assumptions, energy release time being the same, it is possible, albeit with the necessary caution, to ascribe the greater neutron emission from P3 compared to P4 to the fact that r(P3) > r(P4).

8. Conclusions and prospects

From this experiment it can be clearly seen that piezonuclear reactions giving rise to neutron emissions are possible in inert non radioactive solids, in addition to liquids [7-8]. Anyhow, it is also evident that the availability of an amount of stored energy for the reactions exceeding the microscopic nuclear deformed space-time threshold

$$E_{0,\,strong} = 5.888 \times 10^{-8}\ J$$

is not sufficient per se [15]. The energy must be contained in a space and time (and energy) hypervolume such that $r \geq 1$, i.e., such that the phenomenon will actually develop in deformed space-time conditions [6-7]. From Table 2, in fact, it can be seen that it was $\Delta E > E_{0,\,strong}$ in all the test specimens loaded in compression, but r was greater than 1 only in granite test specimens. Hence, even for piezonuclear reactions in solids, the notion of stored energy must be combined with the notion of speed of energy release as is the case for liquids [7].

Another factor to be taken into account is the composition of the materials in which piezonuclear reactions may be produced. It should be noted, in fact, that Carrara marble is basically made of calcite, i.e., a crystalline form of calcium carbonate Ca CO_3, whereas in general granite is made of quartz, alkaline feldspar, plagioclasium and even biotite and horneblend, of which the last two minerals contain iron in greater or lesser quantities. The fact that the marble used in the tests did not contain iron, and granite instead did, could be another factor contributing to the phenomenon in question, by analogy with the case of piezonuclear reactions in liquids. In fact, piezonuclear

reactions with neutron emissions were obtained in liquids containing iron chloride or iron nitrate subjected to ultrasounds and cavitation [7-8]. This could be another factor, together with the speed of energy release, to be considered to account for the emission of neutrons from granite and not from marble, and to open up prospects for future experimental investigations into materials that fail in a catastrophic mode (cusp catastrophe) [9,10]. A subsequent investigation may be conducted both on brittle iron-free materials and on ductile materials containing iron, or on iron itself. Finally, after selecting the materials, it would be necessary to analyse test specimens having different dimensions and slenderness ratios, possibly by setting different piston travel velocities on the testing machine. These studies would contribute to an understanding of the influence of test specimen dimensions and loading rate on neutron emission during fracture.

Acknowledgments

The authors wish to thank A. Zanini, L. Visca and O. Borla (INFN) for their valuable assistance with the neutron detection process. They are also grateful to A. Manuello for his active collaboration to the execution of mechanical compressive tests.

The authors express their gratitude to F. Pistella (former CNR President) for having discussed with them the results of neutron measurements.

References

[1] K. DIEBNER, *Fusionsprozesse mit Hilfe konvergenter Stosswellen – einige aeltere und neuere Versuche und Ueberlegungen*, «Kerntechnik», 3, 1962, pp. 89-93.

[2] S. KALISKI, *Critical masses of miniexplosion in fission-fusion hybrid systems*, «Journal of Technical Phisics», 17, 1976, n. 2, pp. 99-108; IBIDEM, *Bi-conical system of concentric explosive compression of D-T*, 19, 1978, n. 3, pp. 283-289.

[3] F. WINTERBERG, *Autocatalytic fusion-fission implosions*, «Atomenergie-Kerntechnik», 44, 1984, n. 2, pp. 146.

[4] Y. ARATA, Y. ZHANG, *Achievement of solid-state plasma fusion ("cold-fusion")*, «Proceedings of Japan Academy», 71, Ser. B, 1995, n. 10, pp 304-309; IBIDEM, Y. ARATA, H. FUJITA, Y. ZHANG, *Intense deuterium nuclear fusion of pycnodeuterium-lumps coagulated locally within highly deuterated atom clusters*, 78, Ser. B, 2002, n. 7, pp. 201-204.

[5] R. P. TALEYARKHAN, C. D. WEST, J. S. CHO, R. T. LAHEY Jr., R. I. NIGMATULIN, R. C. BLOCK, *Evidence for nuclear emissions during acoustic cavitation*, «Science», 295, 2002, pp. 1868-1873.

[6] F. CARDONE, R. MIGNANI, *Piezonuclear reactions and Lorenz invariance breakdown*, «International Journal of Modern Physics E, Nuclear Physics», 15, 2006, n. 901, pp. 911-924.

[7] F. CARDONE, R. MIGNANI, *Deformed Spacetime*, Springer, Dordrecht, 2007, chaps 16-17.

[8] F. CARDONE et al.: http://www.arxiv.org/abs/0710.5115; http://www.arxiv.org/abs/0812.1272

[9] A. CARPINTERI, *Cusp catastrophe interpretation of fracture instability*, «Journal of the Mechanics and Physics of Solids», 37, 1989, n. 5, pp. 567-582.

[10] A. CARPINTERI, *A catastrophe theory approach to fracture mechanics*, «International Journal of Fracture», 44, 1990, n. 1, pp. 57-69.

[11] G. FERRO, A. CARPINTERI, *Effect of specimen size on the dissipated energy density in compression*, «Journal of Applied Mechanics», 75, 2008, n. 4, 041003, pp 1-8.

[12] J.A. HUDSON, S.L. CROUCH, C. FAIRHURST, *Soft, stiff and servo-controlled testing machines: a review with reference to rock failure*, «Engineering Geology», 6, 1972, pp. 155-189.

[13] RILEM TC 148-SSC, *Test method for measurement of the strain-softening behaviour of concrete under uniaxial compression*, «Materials and Structures», 33, 2000, pp. 347-351.

[14] A. CARPINTERI, M. CORRADO, *An extended (fractal) overlapping crack model to describe crushing size-scale effects in compression*, «Engineering Failure Analysis», 16, 2009, n. 8, pp. 2530-2540.

[15] F. CARDONE, R. MIGNANI, *Energy and Geometry*, World Scientific, Singapore, 2004, chap. 10.

Testo definitivo pervenuto in redazione il 10 dicembre 2008.